Journal Pre-proofs

Discovery of 5-(4-Methylpiperazin-1-yl)-2-nitroaniline Derivatives as A New Class of SIRT6 Inhibitors

Weining Sun, Xiuli Chen, Shenzhen Huang, Wenpei Li, Chenyu Tian, Shengyong Yang, Linli Li

PII: S0960-894X(20)30315-2
DOI: https://doi.org/10.1016/j.bmcl.2020.127215
Reference: BMCL 127215

To appear in: *Bioorganic & Medicinal Chemistry Letters*

Received Date: 28 January 2020
Revised Date: 21 April 2020
Accepted Date: 23 April 2020

Please cite this article as: Sun, W., Chen, X., Huang, S., Li, W., Tian, C., Yang, S., Li, L., Discovery of 5-(4-Methylpiperazin-1-yl)-2-nitroaniline Derivatives as A New Class of SIRT6 Inhibitors, *Bioorganic & Medicinal Chemistry Letters* (2020), doi: https://doi.org/10.1016/j.bmcl.2020.127215

Discovery of 5-(4-Methylpiperazin-1-yl)-2-nitroaniline Derivatives as A New Class of SIRT6 Inhibitors

Weining Sun[a,c], Xiuli Chen[b,c], Shenzhen Huang[b], Wenpei Li[b], Chenyu Tian[a], Shengyong Yang[b], and Linli Li[a,*]

[a]Key Laboratory of Drug Targeting and Drug Delivery System of Ministry of Education, West China School of Pharmacy, Sichuan University, Chengdu, Sichuan 610041, P.R. China

[b]State Key Laboratory of Biotherapy and Cancer Center, West China Hospital, Sichuan University, Chengdu, Sichuan 610041, P.R. China

[c]These authors contributed equally to this work.

*To whom correspondence should be addressed. Key Laboratory of Drug Targeting and Drug Delivery System of Ministry of Education, West China School of Pharmacy, Sichuan University, Chengdu, Sichuan 610041, P.R. China. E-mail: ysylilinli@sina.com.cn.

KEYWORDS: SIRT6, small molecule inhibitor, type 2 diabetes

ABSTRACT

SIRT6 is a deacetylase of histone H3 and inhibitors of SIRT6 have been thought as potential agents for treatment of diabetes. Herein we report the discovery of a series of new SIRT6 inhibitors containing the skeleton 1-phenylpiperazine. Among them, compound 5-(4-methylpiperazin-1-yl)-2-nitroaniline (**6d**) is the most potent one, which showed an IC_{50} value of 4.93 μM against SIRT6 in the Fluor de Lys (FDL) assay. It displayed K_D values of 9.76 μM and 10 μM in surface plasmon resonance (SPR) and isothermal titration calorimetry (ITC) assays, respectively. In selectivity assay, **6d** showed no activity against other members of the HDAC family (SIRT1-3 and HDAC1-11) at concentrations up to 200 μM. In a mouse model of type 2 diabetes, **6d** could significantly increase the level of glucose transporter GLUT-1, thereby reducing blood glucose. Overall, this study provides a promising lead compound for subsequent drug discovery targeting SIRT6.

Sirtuins are NAD^+-dependent lysine deacetylases widespread in prokaryotes and eukaryotes[1,2]. It contains 7 members (SIRT1-SIRT7) in mammals, which have different subcellular localization and biological functions[3]. SIRT6, as a member of the sirtuin family, is closely related to many physiological processes such as developmental retardation[4], DNA repair[5-7], genomic stability[6] and life span[8,9]. Importantly, SIRT6 has been demonstrated to be a corepressor of the transcription factor Hif1α. And knockdown of SIRT6 gene could upregulate glycolysis-related genes, such as GLUT-1, PDK1, ALDOC, and LDH, which are modulated by Hif1α[10]. SIRT6 is thus thought as a potential intervening target for metabolic diseases such as diabetes and obesity.

To date, a number of SIRT6 inhibitors have been reported. Representative compounds are shown in Figure 1, including **5-Cl-PZA**[11], **BMC-12**[12], **EJMC-3**[13], **SYN17739303**[14], and **POA**[11], **JMC-9**[14], and **JMC-16**[14]. Unfortunately, potencies of these compounds are poor (see Figure 1). In addition, most of the SIRT6 inhibitors are multi-target compounds. Therefore, it is of great significance to find SIRT6 inhibitors with potent activity and selectivity at present.

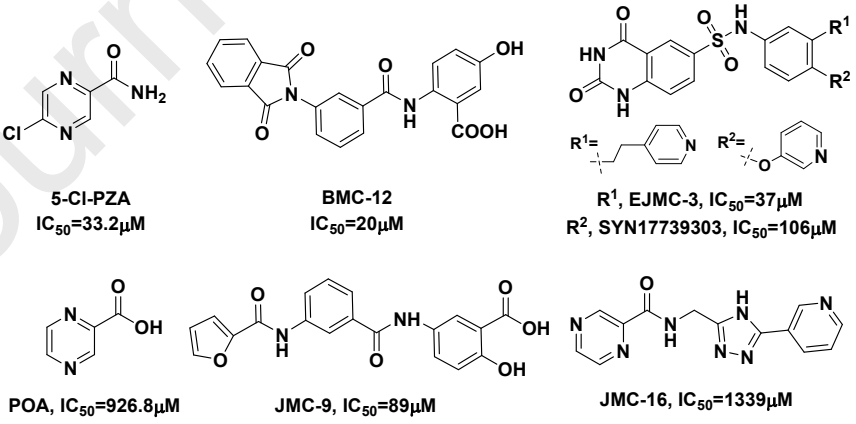

Figure 1. Reported synthetic SIRT6 inhibitors.

To discover new SIRT6 inhibitors, we performed a screening study against our in-house chemical library containing about 2000 compounds by Fluor de Lys (FDL)

assay. Through this screening, a hit compound 1-(4-nitrophenyl)piperazine (**Hit01**, Figure 2A) was obtained, which showed an IC_{50} value of 35 μM (Figure 2B). Further structural optimization was then performed on this compound.

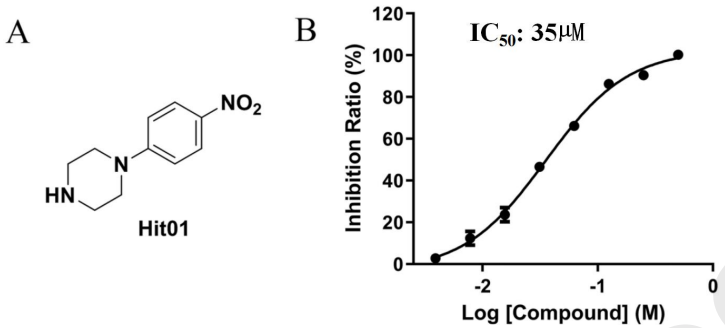

Figure 2. (**A**) Chemical structure of **Hit01**. (**B**) Dose-dependent activities of SIRT6 deacetylation of **Hit01**, determined with acetyl substrate peptide Ac-RYQK(Ac)-AMC. Data are presented as the mean ± s.d., n= 3 wells, from three independent experiments.

The structural optimization of **Hit01** was focused on 1-position piperazine (region I), 3-position (region II) and 4-position (region III) of the phenylpiperazine (Figure 3). Structure-activity relationship (SAR) analyses are based on inhibitory activities of compounds against SIRT6, which were determined by FDL assay. Inhibitory activities of compounds were measured at a single concentration of 300 μM in advance. For compounds with higher potency at 300μM, further IC_{50} values were tested.

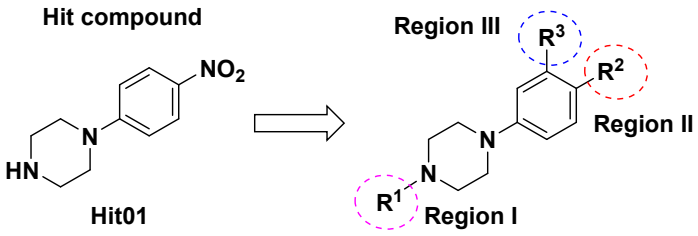

Figure 3. Regions for structural optimization and SAR analyses.

Region I was firstly optimized. To this end, we installed various substituents on the 1-H of piperazine and fixed region II (-NO_2) and III (-H) as their original groups. Six compounds (**PC01-06**) were purchased from the commercial chemical provider Specs. Chemical structures and bioactivities of compounds **PC01-06** are shown in Table 1. All the compounds except **PC06** showed decreased bioactivity against SIRT6. The only compound with activity improved, **PC06**, contains a methyl group at R^1, implying that the methyl group at R^1 is the best choice.

Table 1. Chemical Structures and SIRT6 Inhibitory Activities of Compounds **PC01-06**.

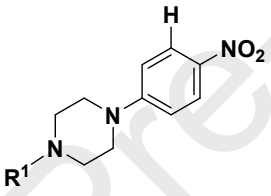

ID	R^1	Inhibition (%) @ 300 μM (IC_{50}/μM)
Hit01	H	81.79 (35.0)
PC01	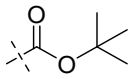	13.07
PC02	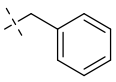	61.70
PC03	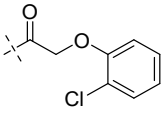	50.69
PC04	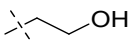	32.01
PC05	-CH_2CH_3	69.67

PC06	-CH_3	112.70 (21.91)

Region II (R^2) was then optimized. For this purpose, region I and III were fixed as –CH_3 and –H, respectively, and region II (R^2, -NO_2) was replaced by various substituents. We purchased nine compounds (**PC07-15**) from Specs. Chemical structures and bioactivities are presented in Table 2. Although various substituents at R^2, bioactivities of the new compounds are still less than that of **PC06**, indicating that a nitro group at R^2 position is suitable.

Table 2. Chemical Structures and SIRT6 Inhibitory Activities of Compounds **PC06-15**.

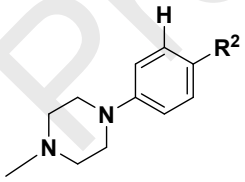

ID	R^2	Inhibition (%) @ 300μM (IC_{50}/μM)
PC06	-NO_2	112.70 (21.91)
PC07	H	35.77
PC08	F	24.31
PC09	-CF_3	45.67
PC10	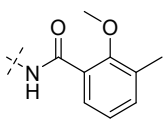	41.64

PC11	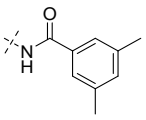	26.24
PC12	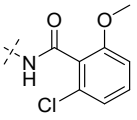	46.68
PC13	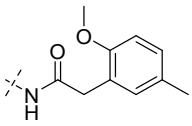	46.86
PC14	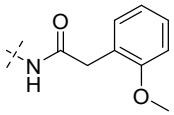	39.13
PC15		22.83

Region III (R^3) was finally optimized. To this end, we synthesized thirteen new 1-methyl-4-(4-nitrophenyl)piperazine derivatives (**6a**-**m**), in which region I and II were fixed as the methyl group and the nitro group, respectively, and region III was changed with various substituent groups. Scheme 1 illustrates synthetic routes for compounds **6a**-**m**. Condensation reactions between 2,4-difluoro-1-nitrobenzene (**3**) or 5-fluoro-2-nitrobenzoic acid (**7**) and various substituted amino (**4a**-**c**, **8a**-**f**) in DMF solution gave compounds **5a**-**c** or **9a**-**f** as intermediates. Final products **6a**-**m** were then obtained from reactions of **2a**-**d**, **5a**-**c**, and **9a**-**f** with commercially available 1-methylpiperazine (**1**).

Scheme 1. Synthesis of compounds **6a**-**m**.[a]

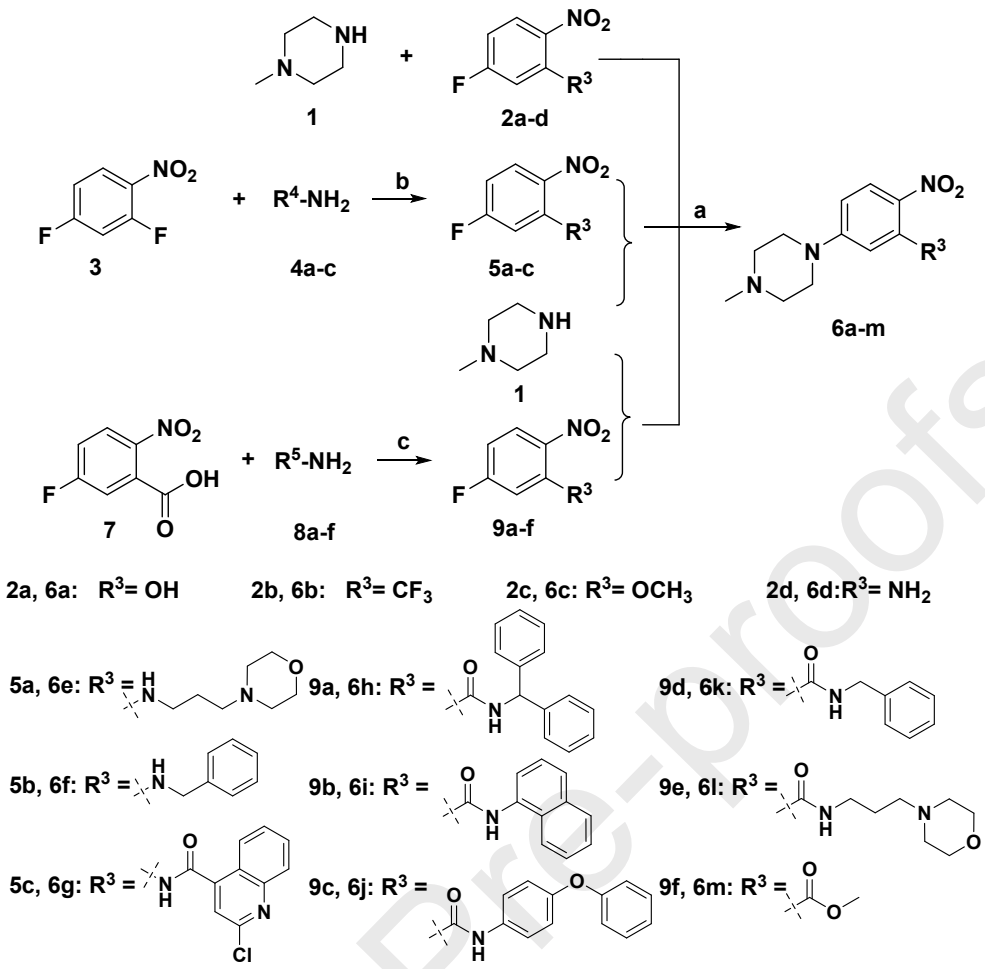

[a] **Reagents and conditions:** a) $Pd(OAc)_2$, Xant-phos, 1,4-dioxane,Cs_2CO_3, 100 °C, 12 h; b): R^4-NH_2, K_2CO_3, DMF, 50 °C, overnight; c) i: $SOCl_2$, 50 °C, 4-5 h; ii: R^5-NH_2, DMAP, DMF, RT, overnight.

Bioactivities of compounds **6a-m** are shown in Table 3. Compounds **6a-d**, which contain smaller subgroups at R^3 (-OH, -CF_3, -OCH_3, -NH_2, respectively), displayed enhanced activity compared with **PC06**. Among them, compound **6d** is the most potent one with an IC_{50} value of 4.93 μM, which bears an amino group at R^3 (Figure 4A). Compounds **6e-g**, having a substituted amino group at R^3, also showed activity but weaker potency compared with **6d**. Compound **6h-m**, which harbor relatively larger substituents, again displayed considerable activity. But their potencies did not exceed that of **6d**. Overall, among all the purchased and synthesized compounds, **6d** is

the most potent one. Further studies were conducted on this compound.

Table 3. Chemical Structures and SIRT6 Inhibitory Activities of Compounds **6a-m**.

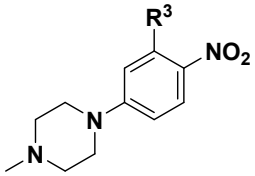

ID	R^3	Inhibition (%) @ 300 μM (IC_{50}/μM)	ID	R^3	Inhibition (%) @ 300 μM (IC_{50}/μM)
PC0	H	112.70 (21.91)	**6a**	-OH	119.1 (11.04)
6b	$-CF_3$	88.3 (21.13)	**6c**	$-OCH_3$	107.8 (9.09)
6d	$-NH_2$	107.20 (4.93)	**6e**	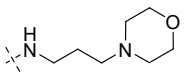	63.70
6f	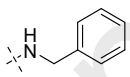	96.00 (12.49)	**6g**	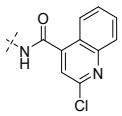	97.08 (12.37)
6h	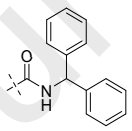	85.10	**6i**	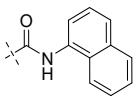	97.10 (16.82)
6j	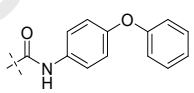	87.50 (20.94)	**6k**	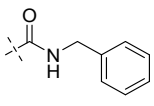	108.00 (17.53)
6l	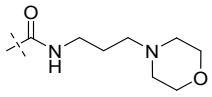	82.30	**6m**		100.90 (9.46)

Several other methods including differential scanning fluorimetry (DSF) assays,

surface plasmon resonance (SPR) assays and isothermal titration calorimetry (ITC) assays were used to validate the bioactivity of compound **6d**. In the DSF assay, **6d** showed an ability to shift the melting temperature (T_m) with $\triangle T_m$ = 1.88 °C at a concentration of 40 μM (Figure 4B). In the SPR assay, **6d** displayed a K_D value of 9.76 μM (Figure 4C and 4D). In the ITC assay, **6d** showed an K_D value of 10.00 μM (Figure 4E). All of these reuslts verified the bioactivity of **6d**.

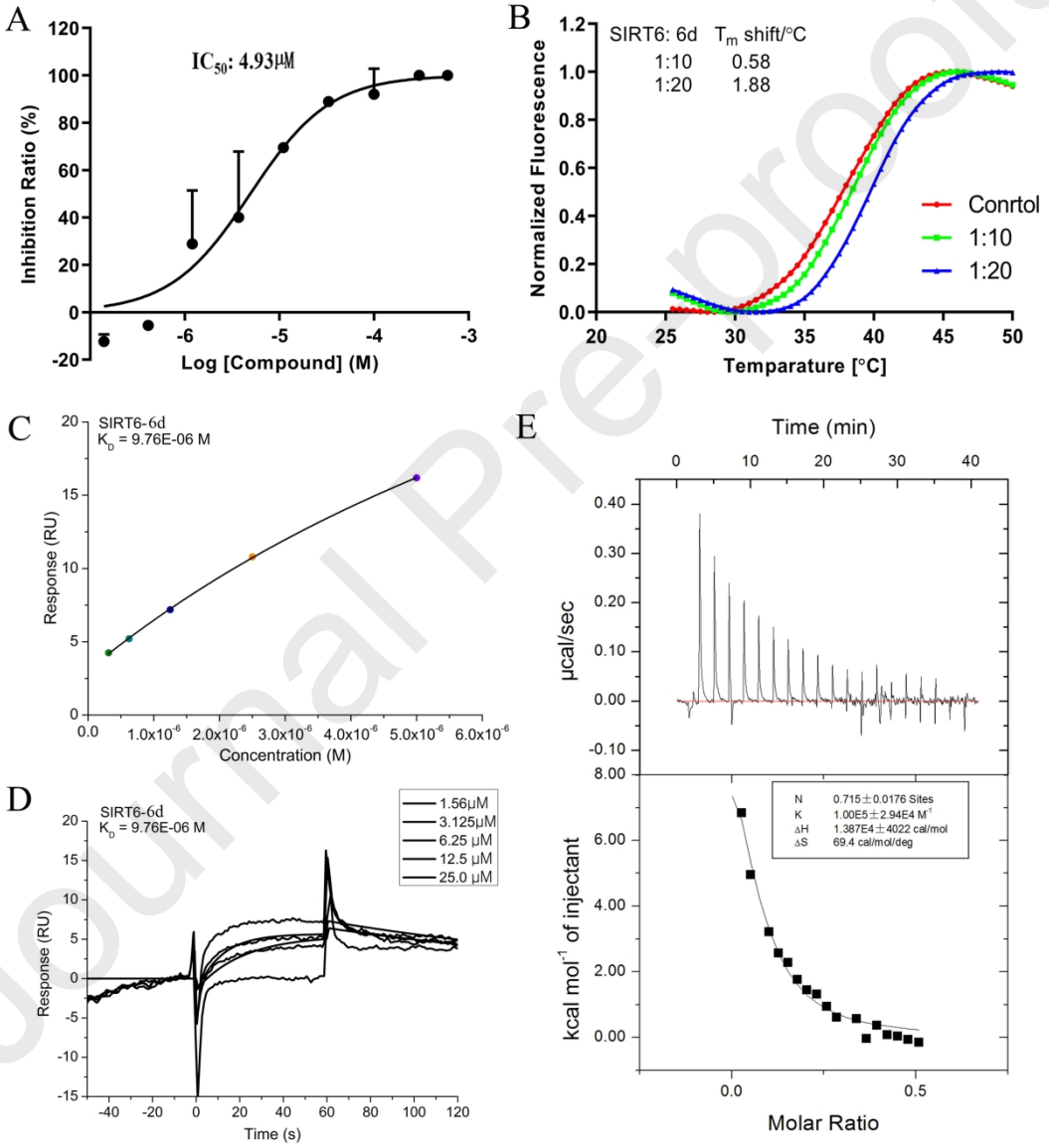

Figure 4. Bioactivity verification of compound **6d** by FDL, DSF, SPR, and ITC assays. (**A**) Dose-dependent activities of SIRT6 deacetylation of **6d**, determined with acetyl substrate peptide Ac-RYQK(Ac)-AMC. Data are presented as the mean ± s.d.,

n= 3 wells, from three independent experiments. (**B**) The effect of **6d** on the thermal stability of SIRT6 was detected using DSF. (**C**, **D**) The binding curve and steady-state evaluation of **6d** binding to SIRT6 using SPR. (**E**) ITC binding curves for SIRT6 and **6d**.

To examine the selectivity of **6d**, we measured the bioactivity of **6d** against 14 other deacetylases including SIRT1-3 and HDAC1-11 by FDL assays. The results showed that **6d** did not exhibit inhibitory activity against the tested deacetylases at concentrations up to 200 μM, implying a good selectivity (Table 4).

Table 4. Target selectivity of **6d** among HDAC family enzymes [a]

Protein	IC_{50} (μM)	Protein	IC_{50} (μM)
SIRT1	>200	HDAC5	>200
SIRT2	>200	HDAC6	>200
SIRT3	>200	HDAC7	>200
SIRT6	4.93	HDAC8	>200
HDAC1	>200	HDAC9	>200
HDAC2	>200	HDAC10	>200
HDAC3	>200	HDAC11	>200
HDAC4	>200		

[a]The activity of **6d** against SIRT6 was determined by the FDL assay with acetyl substrate peptide Ac-RYQK(Ac)-AMC.

To evaluate the inhibition effect of **6d** on SIRT6 deacetylation in intact cells, we monitored the acetylation status of H3K9 and H3K18 in BxPC-3 cells treated with **6d**

at different concentrations; H3K9 and H3K18 were selected because they are known targets of SIRT6. It was found that **6d** increased the level of both H3K9ac and H3K18ac in a dose-dependent manner, suggesting that **6d** is active in cultured cells (Figure 5A).

Finally, western blot assay was performed to examine the effect of **6d** on the level of glucose transporter GLUT-1. In this assay, BxPC-3 cells were used again. As shown in Figure 5B, **6d** could increase the GLUT-1 expression in a dose-dependent manner. In a mouse model of type 2 diabetes (T2D, in high-fat-diet-fed animals), **6d** could significantly reduce the blood glucose content, and has no effect on the body weight of mice (Figure 5C and 5D). In normal mice, **6d** had no impact on blood glucose or body weight (Figure S1 A, B).

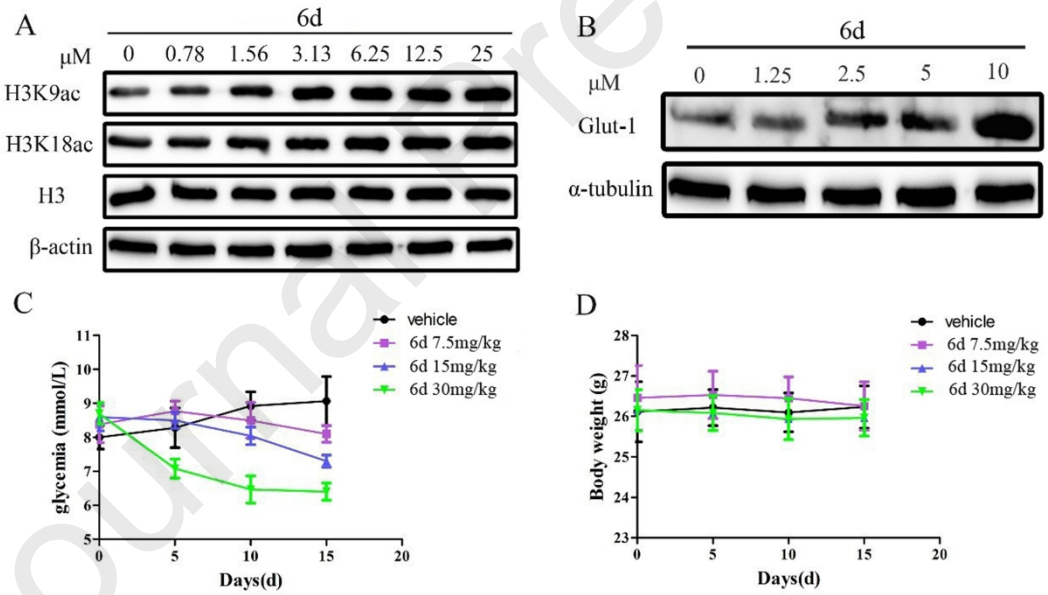

Figure 5. (**A**) Western blot analysis of H3K9ac and H3K18ac protein expression in BxPC-3 cells treated with 0.78, 1.56, 3.13, 6.25, 12.5, and 25 μM **6d** for 48 h. β-actin, loading control. (**B**)Western blot analysis of GLUT1 protein expression in BxPC-3 cells treated with 1.25, 2.5, 5, and 10 μM **6d** for 72 h. α-tubulin, loading control. (**C**) The changes of blood glucose were observed in a mouse model of T2DM after intraperitoneal injection of **6d**. (**D**) The changes of body weight were observed in a

mouse model of T2DM after intraperitoneal injection of **6d**.

In summary, we discovered a number of new SIRT6 inhibitors containing the skeleton 1-phenylpiperazine. Compound **6d** is the most potent one, which showed an IC_{50} value of 4.93 μM in FDL assays, and K_D values of 9.76 μM and 10 μM in SPR and ITC assays, respectively. In BxPC-3 cells, **6d** could increase both H3K9ac and H3K18ac levels in a concentration-dependent manner, and upregulate the expression of glucose transporter GLUT1. In vivo, **6d** also showed efficacy in a mouse model of T2D. Collectively, **6d** could be a potential lead compound for further drug discovery targeting SIRT6.

Acknowledgements

This work was supported by the National Natural Science Foundation of China (21772130), National Science and Technology Major Project (2018ZX09711002-011-019, 2018ZX09201018, and 2019ZX09301-135), and 1.3.5 project for disciplines of excellence, West China Hospital, Sichuan University.

REFERENCES

1. Bonkowski M S, Sinclair D A. Slowing ageing by design: the rise of NAD^+ and sirtuin-activating compounds. *Nature reviews Molecular cell biology*, 2016, 17(11): 679

2. Sauve A A, Wolberger C, Schramm V L, et al. The biochemistry of sirtuins. *Annu. Rev. Biochem.*, 2006, 75: 435-465.

3. Blander G, Guarente L. The Sir2 family of protein deacetylases. *Annual review of biochemistry*, 2004, 73(1): 417-435.

4. Zhang W, Wan H, Feng G, et al. SIRT6 deficiency results in developmental retardation in cynomolgus monkeys. *Nature*, 2018, 560(7720): 661.

5. Mao Z , Hine C , Tian X , et al. SIRT6 Promotes DNA Repair Under Stress by Activating PARP1. *Science*, 2011, 332(6036):1443-1446.

6. Mostoslavsky R, Chua K F, Lombard D B, et al. Genomic instability and aging-like phenotype in the absence of mammalian SIRT6. *Cell*, 2006, 124(2): 315-329.

7. Kaidi A, Weinert B T, Choudhary C, et al. Human SIRT6 promotes DNA end resection through CtIP deacetylation. *Science*, 2010, 329(5997): 1348-1353.

8. Kawahara T L A, Michishita E, Adler A S, et al. SIRT6 links histone H3 lysine 9 deacetylation to NF-κB-dependent gene expression and organismal life span. *Cell*, 2009, 136(1): 62-74.

9. Kanfi Y, Naiman S, Amir G, et al. The sirtuin SIRT6 regulates lifespan in male mice. *Nature*, 2012, 483(7388): 218.

10. Zhong L, D'Urso A, Toiber D, et al. The histone deacetylase Sirt6 regulates glucose homeostasis via Hif1α. *Cell*, 2010, 140(2): 280-293.

11. Bolívar B E, Welch J T. Studies of the binding of modest modulators of the human enzyme, sirtuin 6, by STD NMR. *ChemBioChem*, 2017, 18(10): 931-940.

12. Damonte P, Sociali G, Parenti M D, et al. SIRT6 inhibitors with salicylate-like structure show immunosuppressive and chemosensitizing effects. *Bioorganic & medicinal chemistry*, 2017, 25(20): 5849-5858.

13. Sociali G, Galeno L, Parenti M D, et al. Quinazolinedione SIRT6 inhibitors sensitize cancer cells to chemotherapeutics. *European journal of medicinal chemistry*, 2015, 102: 530-539.

14. Parenti M D, Grozio A, Bauer I, et al. Discovery of novel and selective SIRT6 inhibitors. *Journal of medicinal chemistry*, 2014, 57(11): 4796-4804.

Graphical abstracts

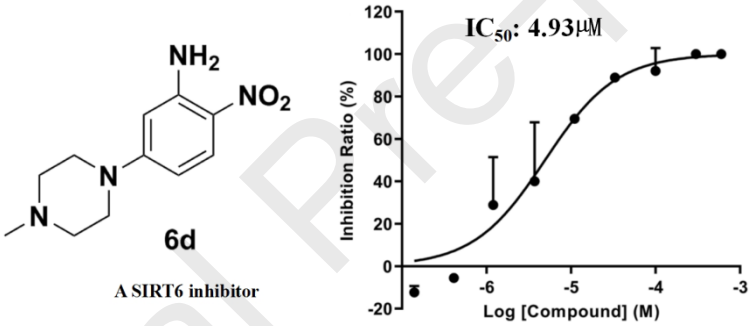

Declaration of interests

☒ The authors declare that they have no known competing financial interests or personal relationships that could have appeared to influence the work reported in this paper.

☐The authors declare the following financial interests/personal relationships which may be considered as potential competing interests: